

RESEARCH PAPER



C7 peptide inhibits hepatocellular carcinoma metastasis by targeting the HGF/c-Met signaling pathway

Mingyuan Zhao^{a*}, Yinhe Wang^{a,b*}, Yan Liu^a, Wanchun Zhang^{a,b}, Yakun Liu^a, Xiaoming Yang^c, Yunxia Cao^{a,b}, and Siying Wang^{ib}^a

^aDepartment of Pathophysiology, Anhui Medical University, Hefei, Anhui, P. R. China; ^bDepartment of Gynaecology and Obstetrics, The First Affiliated Hospital of Anhui Medical University, Hefei, Anhui, P. R. China; ^cState Key Laboratory of Proteomics, Beijing Proteome Research Center, National Center for Protein Sciences (Beijing), Beijing Institute of Lifeomics, Beijing, P. R. China

ABSTRACT

Hepatocellular carcinoma (HCC), characterized by a high rate of metastasis and recurrence after surgery, is caused by malignant proliferation of hepatocytes with epigenetic and/or genetic mutations. In particular, abnormal activation of the hepatocyte growth factor (HGF)/c-mesenchymal-epithelial transition receptor (c-Met) axis is closely associated with HCC metastasis. Unfortunately, effective treatments or drugs that target the HGF/c-Met signaling pathway are still in the research pipeline. Here, a c-Met inhibitor named the C7 peptide, which can inhibit both HGF and c-Met, can significantly inhibit HGF-induced (but not EGF-induced) cell migration and suppress the phosphorylation of c-Met, Akt and Erk1/2. Moreover, the C7 peptide can also significantly suppress tumor metastasis in nude mice and the phosphorylation of c-Met. Together, our current findings, demonstrated that the C7 peptide can inhibit HGF-induced cancer cell migration and invasion through the inhibition of Akt and Erk1/2. Identification of a peptide that can block HGF/c-Met signaling provides new insight into the mechanism of HCC and future clinical treatments.

ARTICLE HISTORY

Received 28 February 2019
Revised 23 April 2019
Accepted 23 June 2019

KEYWORDS

C7 peptide; hepatocellular carcinoma (HCC); HGF/c-Met axis; migration; invasion

Introduction

Hepatocellular carcinoma is common primary cancer with high incidence and mortality throughout the world.¹ Surgical resection combined with radiotherapy, chemotherapy or targeted drugs remains the primary treatment for early HCC.² However, after treatment, patients with advanced HCC usually suffer from local recurrence and even metastasis, and these patients generally have a very poor prognosis with a low 5-year relative survival rate.³ It has been reported that high expression of c-Met was found in various cancers, especially in hepatocellular carcinoma.⁴ C-Met, a trans-membrane tyrosine kinase receptor, is frequently associated with the process of tumor growth, invasion and migration.⁵ Hepatocyte growth factor (HGF), a unique physiological ligand of c-Met, also plays a significant role in tumor progression.^{6,7} The HGF/c-Met axis is thought to be regulated by various mechanisms under normal circumstances and activates the PI3K/Akt and Erk1/2 signaling pathway cascades, which play a vital role in mediating HGF-induced invasion and metastasis of tumor cells.^{8,9} Based on these characteristics, c-Met and HGF have been deemed to be ideal therapeutic targets in cancer treatments.¹⁰ In recent years, numerous inhibitors targeting the HGF/c-Met axis have entered the preclinical phase or clinical evaluation.¹¹

Rilotumumab is the first monoclonal antibody that selectively targets HGF to enter phase III clinical trials.¹² Furthermore, some receptor tyrosine kinase inhibitors

(TKIs) are significant components of c-Met targeting agents. Cabozantinib, a multiple target c-Met kinase inhibitor, has achieved remarkable results in phase 3 clinical trials of patients with advanced hepatocellular carcinoma.¹³ In our laboratory, we found that SU5416 is a potent inhibitor of Met and can block HGF-induced cell invasion.¹⁴ These findings demonstrate the importance of HGF/c-Met signaling pathways in tumor development. While antibodies and TKIs have clinical advantages and can effectively inhibit the HGF/c-Met signaling pathway, they have some deficiencies in clinical application. Patients receiving these therapies targeting HGF or c-Met proteins still have high mortality rates and resistance to chemotherapy, immunotherapy or hormonal therapy.¹⁵ Therefore, the development of new targeted drugs and rational combination therapeutic strategies are necessary to maintain a pool of effective treatment at all times. Targeting peptides are characterized by biomolecules with lower molecular weights, specific sequences and good organizational penetration abilities, emerging as attractive or important therapeutic agents.¹⁶ For example, the designed peptide (referred to as VGB4) indicates that VGB4 may be applicable for anti-angiogenic and antitumor therapy.¹⁷ Therefore, peptide-targeted therapy has great prospects of development.

Our results identified a small peptide fragment that targets c-Met from the cDNA gene bank by the phage display technique. Since the inserted peptide was directly opposite to the

CONTACT Yunxia Cao  caoyunxia6@126.com  Department of Gynaecology and Obstetrics, The First Affiliated Hospital of Anhui Medical University, 218 JiXin Road, Hefei, Anhui 230032, P. R. China; Siying Wang  sywang@ahmu.edu.cn  Department of Pathophysiology, Anhui Medical University, 81 MeiShan Road, Hefei, Anhui 230032, P. R. China.

*These authors contributed equally to this work.

 Supplemental data for this article can be accessed on the [publisher's website](#).

coding gene, the corresponding coding gene was obtained by sequencing, and the amino acid sequence was deduced. We obtained a peptide candidate that consists of 7- amino acids, named the C7 peptide, which exhibited a moderate affinity and good specificity for binding to Met.

Results

Identification of peptides that bind c-Met from phage libraries

To screen for peptide sequences that specifically bind to c-Met, we screened the T7 select Human Liver Tumor cDNA Library and the Ph.D-C7CTM phage display peptide library. The biopanning method refers to the processes of screening peptides with a high affinity for a target material, and a schematic illustration is shown (Figure 1a). After four rounds of screening, the results showed that M13 phage was significantly enriched and the titer of the phage increased from 2.0×10^4 to 1.7×10^5 pfu/ μ l (Table 1). In each round of screening, the plates were not coated with c-Met protein or with s-Protein as negative controls. The P/N value (the ratio of the phage titer of the c-Met extracellular domain protein to the phage titer of the corresponding negative control) was measured after the screening process. As the screening intensity increased, the P/N value increased gradually. The P/N value of M13 phage from the Ph.D-C7CTM phage display

peptide library increased from 2.8 to 24.6. The P/V value of T7 phage increased from 3.6 to 17.0 (Supplementary Table 1), which indicated that the high-affinity phages specifically binding to c-Met were well enriched, and M13 phage was named Met-M13.

Binding activity of Met-M13 to c-Met

To investigate whether Met-M13 actually bound to the c-Met protein, we directly coated the enzyme-linked plate with c-Met extracellular domain protein to detect the binding activity of gradient-diluted Met-M13 phage and negative control phage to the c-Met extracellular domain protein by ELISA assay. As a result, we found that the binding activity of Met-M13 phage to c-Met was markedly increased with increasing phage titer (Table 2). In the presence of a high titer of Met-M13 phage, the Met-M13 phage binding activity, expressed as an optical density (OD) value, was twice the value of that of Cont-M13 (Table 2). We also obtained the same results using the HepG2 cell line (Supplementary Table 2).

Single-strand DNA sequencing of M13 phage and peptide synthesis

The eluted high-affinity phages from rounds 3–4 were amplified by incubation with ER2738 host cells. The phage peptide sequence was analyzed by sequencing the phage plasmid

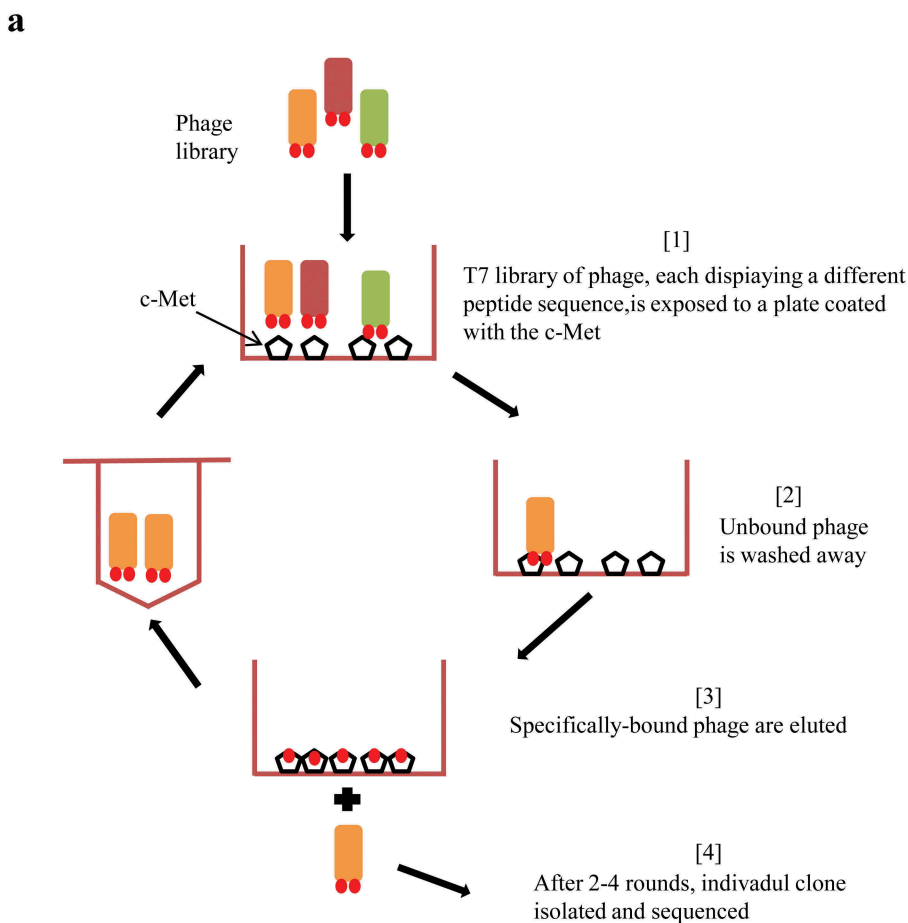


Figure 1. Schematic illustration of c-Met targeting peptide screening.

Table 1. Enriching of the target phage (Pfu/ μ l).

Rounds	1	2	3	4
c-Met (M13 Phage)	2.0×10^4	1.5×10^5	1.0×10^5	1.7×10^5
Control	7.0×10^3	7.5×10^3	7.4×10^3	6.9×10^3
c-Met (T7 Phage)	4.0×10^2	8.0×10^2	2.3×10^3	1.7×10^3
S-Protein (T7 Phage)	1.1×10^2	1.2×10^2	1.1×10^2	1.0×10^2

ssDNA. The sequence results proved there was a single sequence, and the peptide was speculated. The functional sequence of the amino acid is 3'-TPQTRPN-5' (Table 3). To ensure the stability and purity of the peptide, cysteine was added at the 3' and 5' terminus of the sequence to form a disulfide bond bridge. Thereby, the sequence became 3'-CTPQTRPNC-5', was synthesized with a purity of more than 99%, and was named the C7 peptide (Table 3).

C7 peptide inhibits HGF-induced scatter of liver cancer cells

HGF can mediate the mobility of epidermal cells as a scatter factor,¹⁸ therefore scatter assay was used to assess the optimal experimental concentration and inhibitory effect of the C7 peptide. The results showed that HGF had an obvious effect on cell scatter at a concentration of 20 ng/ml (Supplementary Figure 1a). We also explored the optimal inhibition concentration of the C7 peptide and concentrations of 100 ng/ml and 150 ng/ml significantly inhibited HepG2 cell scatter induced by HGF 20ng/ml (Supplementary Figure 1a). In subsequent biological behavior experiments, we will apply the concentration that was explored. In the experimental design, epidermal growth factor (EGF) was added as the control group, which also contributes considerably to the scatter and migration in HCC.¹⁹ The results of the scatter assay showed that the C7 peptide exerted a potent inhibitory effect on the scatter of HepG2, Hep3B and HCCLM3 cells. However, the C7 peptide did not inhibit EGF-mediated cell division (Figure 2a).

HGF does not promote HCC cells proliferation and the C7 peptide inhibits HGF-induced growth in HUVEC cells

HGF not only promotes the proliferation of normal hepatocytes and vascular endothelial cells,¹⁴ but also promotes the growth of many tumor cell lines.^{20,21} However, proliferation effect of HGF on liver cancer cell lines is currently controversial. It is reported that HGF can not promote the DNA synthesis of liver cancer.^{22,23} To study the effects of HGF on hepatoma cell lines and human umbilical vein endothelial cells (HUVEC), ability of

cell proliferation after HGF treatment was detection using MTT assay. In this experiments, results showed that HGF promoted HUVEC cells proliferation (Figure 3a). However, HepG2 and Hep3B cells were treated with 20 ng/ml and 40 ng/ml HGF, and the effect of HGF was very weak (Figure 3a). HGF-induced proliferation was inhibited by the C7 peptide that did not inhibit EGF-induced proliferation in HUVEC cells (Figure 3b). Owing to HGF had little effect on HepG2 and Hep3B cells proliferation (Figure 3c-d), so the inhibitory effect of the C7 on HGF-induced proliferation was unable to evaluate in HCC cell lines.

C7 peptide inhibits HGF-induced motility and migration of liver cancer cells

The HGF/c-Met axis has been demonstrated to be associated with cell a metastasis phenotype.²⁴ Therefore, we explored the inhibitory activity of the C7 peptide on cell mobility in HepG2, Hep3B, HCCLM3 cells induced by HGF using routine artificial wound closure and migration assays. When a wound was introduced into subconfluent cells, more cells migrated across the wound in cells supplemented with HGF or EGF compared to those in the control group after 24 h. However, the C7 peptide had a potential inhibitory effect on motility in cells induced by HGF and no effect on EGF-mediated cell motility (Supplementary Figure 2a). Likewise, the effect of c-Met inhibition by the C7 peptide on cell migration was evaluated by transwell assay. The findings demonstrated that the addition of the C7 peptide resulted in significantly less HGF-treated cells migrating through the porous membrane; however, this phenomenon did not occur in EGF-induced cells (Figure 2b-c). The same results were observed in HepG2, Hep3B and HCCLM3 cells.

C7 peptide inhibits HGF-induced invasion of liver cancer cells

HGF/Met signaling has been associated with tumor progression towards an invasive-metastatic phenotype known as 'invasive growth'.²⁵ Transwell chambers and Matrigel have been used to evaluate the features. The results of invasion assays showed that the C7 peptide had a potential inhibitory effect on invasion induced by HGF; however, the C7 peptide had no effect on EGF-mediated cell invasion (Figure 2d-e). The same results were obtained in HepG2, Hep3B and HCCLM3 cells.

Table 2. Conjugation of Met-M13 with extracellular protein of c-Met.

	M13 Phage (Pfu/ μ l)					
	1.0×10^{12}	2.0×10^{11}	4.0×10^{10}	8.0×10^9	1.6×10^9	3.2×10^8
Met-M13	$0.89 \pm 0.07^{**}$	$0.26 \pm 0.08^{**}$	$0.07 \pm 0.05^{**}$	0.03 ± 0.02	0.01 ± 0.01	0.01 ± 0.01
Con-M13	0.34 ± 0.01	0.12 ± 0.08	0.03 ± 0.04	0.01 ± 0.01	0.01 ± 0.01	0.01 ± 0.01

Measurement data were presented as mean \pm standard deviation, ** $P < 0.01$

Table 3. The information of the C7 peptide.

Peptide	Functional Sequence	Modified Sequence	Purity	Molecular Weight
C7 peptide	TPQTRPN	CTPQTRPNC	99.68%	1017.16

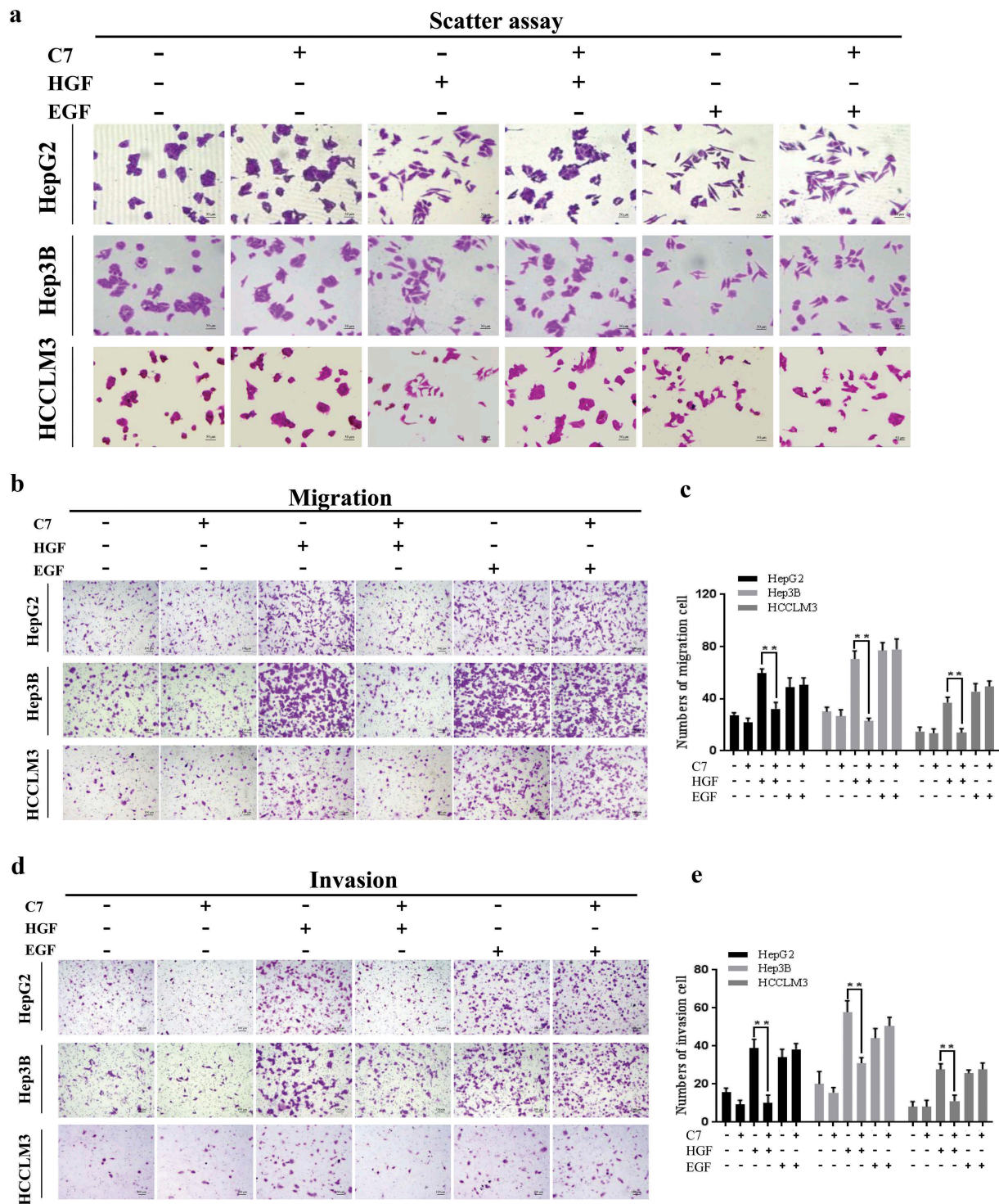


Figure 2. Effect of the C7 peptide on HGF-induced cellular functions.

(a) Measurement of cell scatter treated with C7 coupled with or without HGF and EGF in HepG2, Hep3B and HCCLM3 cells for 24 h, magnification $\times 200$. (b) Representative photographs of the transwell assay, magnification $\times 100$. (c) The statistical result of cell migration in three cells. (d) Representative photographs of representative quantifications of cells that had invaded through the Matrigel and pores, magnification $\times 100$. (e) The statistical result of cell invasion in three cells. C7:100 $\mu\text{g/ml}$, HGF: 20 ng/ml , EGF: 10 ng/ml . $**P < .01$. All viable cells were visualized using crystal violet staining and photographed. At least three independent experiments were performed.

C7 peptide inhibits the HGF/c-Met signaling pathway in liver cancer cells

Above evidences suggested that the C7 peptide can inhibit cancer cell invasion and migration. To investigate whether HGF/c-Met signaling is involved, we detected the phosphorylation level of its

downstream signaling proteins by Western blot. The results showed that c-Met was phosphorylated within 15 min after HGF stimulation in HepG2 and Hep3B cells. However, c-Met was not phosphorylated by EGF stimulation, and the C7 peptide only attenuated the level of phospho-Met induced by HGF in

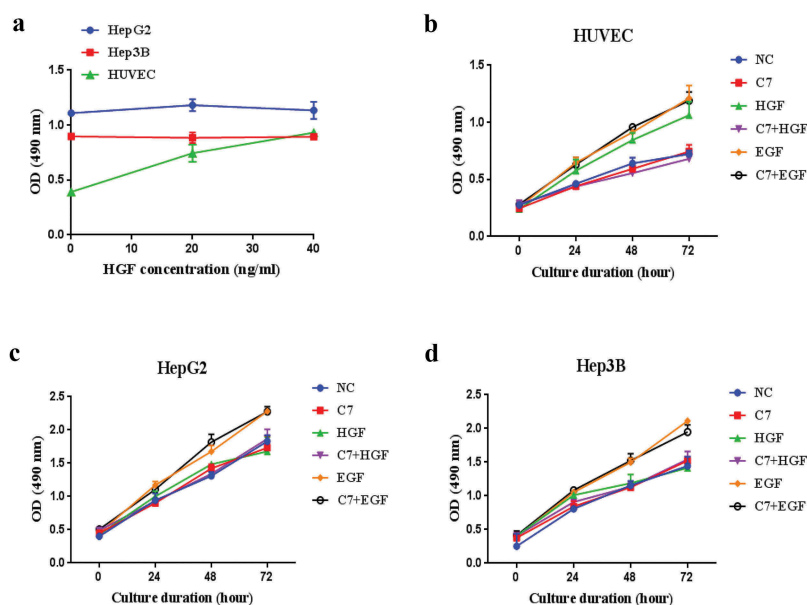


Figure 3. Effects of HGF or C7 peptide on cells growth.

(a) HUVEC, HepG2 and Hep3B cells were cultured in the presence of HGF at 0, 20 and 40 ng/ml. (b&c&d) HUVEC, HepG2 and Hep3B cells were cultured in serum-reduced media and treated with C7 peptide, HGF and EGF for 24–72 h. C7: 100 μ g/ml, HGF: 20 ng/ml, EGF: 10 ng/ml. Each value represents the mean \pm SD of triplicate measurements.

HepG2 (Figure 4a–b) and Hep3B cells (Figure 4c–d). Akt and Erk1/2 were phosphorylated by HGF and EGF (Figure 4e–h). Although the C7 peptide attenuated the level of phospho-Akt and phospho-Erk1/2 induced by HGF, it did not attenuate the protein phosphorylation level induced by EGF (Figure 4e–h). This result demonstrated that EGF did not promote cell migration and invasion through the HGF/c-Met signaling pathway. It's reported that binding of EGF to epidermal growth factor receptor (EGFR) activates RAF/MEK/ERK and PI3K/Akt pathways, which plays a crucial role in both tumor migration and invasion.¹⁵ Therefore, the C7 peptide inhibited the phosphorylation of c-Met and the downstream proteins Akt and Erk1/2 induced by HGF, which had no effect on phospho-Akt and Erk1/2 by EGF.

C7 peptide competitively inhibits the binding of HGF to c-Met

Our previous data demonstrated that the C7 peptide specifically blocked c-Met phosphorylation. There are many ways to activate c-Met protein, including the phosphorylation of c-Met via binding to HGF and the spontaneous phosphorylation of c-Met when it was overexpressed.²⁶ Competition experiments were designed to explore how the C7 peptide inhibits phosphorylation of c-Met. In this experiment, when the concentration of HGF was 20 ng/ml, the effect of the C7 peptide on blocking the phosphorylation of c-Met, Akt, and Erk1/2 induced by HGF became more obvious with increasing concentrations of the C7 peptide in HepG2 and Hep3B cells (Figure 5a–d). Furthermore, when the cells were stimulated with the C7 peptide at a concentration of 100 μ g/ml, the ability of the C7 peptide to block c-Met, Akt, Erk1/2 phosphorylation that was induced by increased HGF concentration became weaker (Figure 5e–h). The results showed that the C7 peptide blocked c-Met phosphorylation by blocking the binding of HGF to c-Met.

C7 peptide inhibited tumor metastasis in vivo

To confirm the inhibition of the C7 peptide *in vivo*, we designed orthotopic xenograft models in nude mice using the HCCLM3 cell line. The tumor-bearing mice were intravenously administered 10 mg/kg C7 peptide or PBS once every two days 20 times, starting two days after transplantation. In animal experiments, the result showed that the number of lung metastatic nodules in the C7 peptide group was less than that in the control group (Figure 6a–b). H&E staining also showed the same result (Figure 6c). Immunohistochemistry demonstrated that the level of phospho-Met and phospho-Erk was higher in the C7 peptide group than in the control group (Figure 7a).

Discussion

The HGF/c-Met axis is a pivotal component in physiological invasive growth and wound healing processes.^{27,28} The disorder of this pathway drives the malignant progression of various tumors.²⁹ This indicates that targeting the HGF/c-Met signaling pathway is a potential targeted therapeutic strategy in cancer treatment. Our results revealed the C7 peptide exhibited a moderate affinity and good specificity for binding to c-Met on the surface of phages. The C7 peptide can inhibit cell migration and invasion *in vivo* and *in vitro* by inhibiting the Akt and Erk1/2 signaling pathways.

According to the report from Lisha Chen et al in 2015, an HGF inhibitory peptide named HGP-1 was found, which has a 15-amino acid sequence.³⁰ In our study, the C7 peptide had only a 7-amino acid sequence. To maintain the stability and purity of the C7 peptide in subsequent experiments, two cysteines were added at the 3' and 5' terminus of the sequence. Interesting, the C7 peptide can be dissolved in ultra-pure

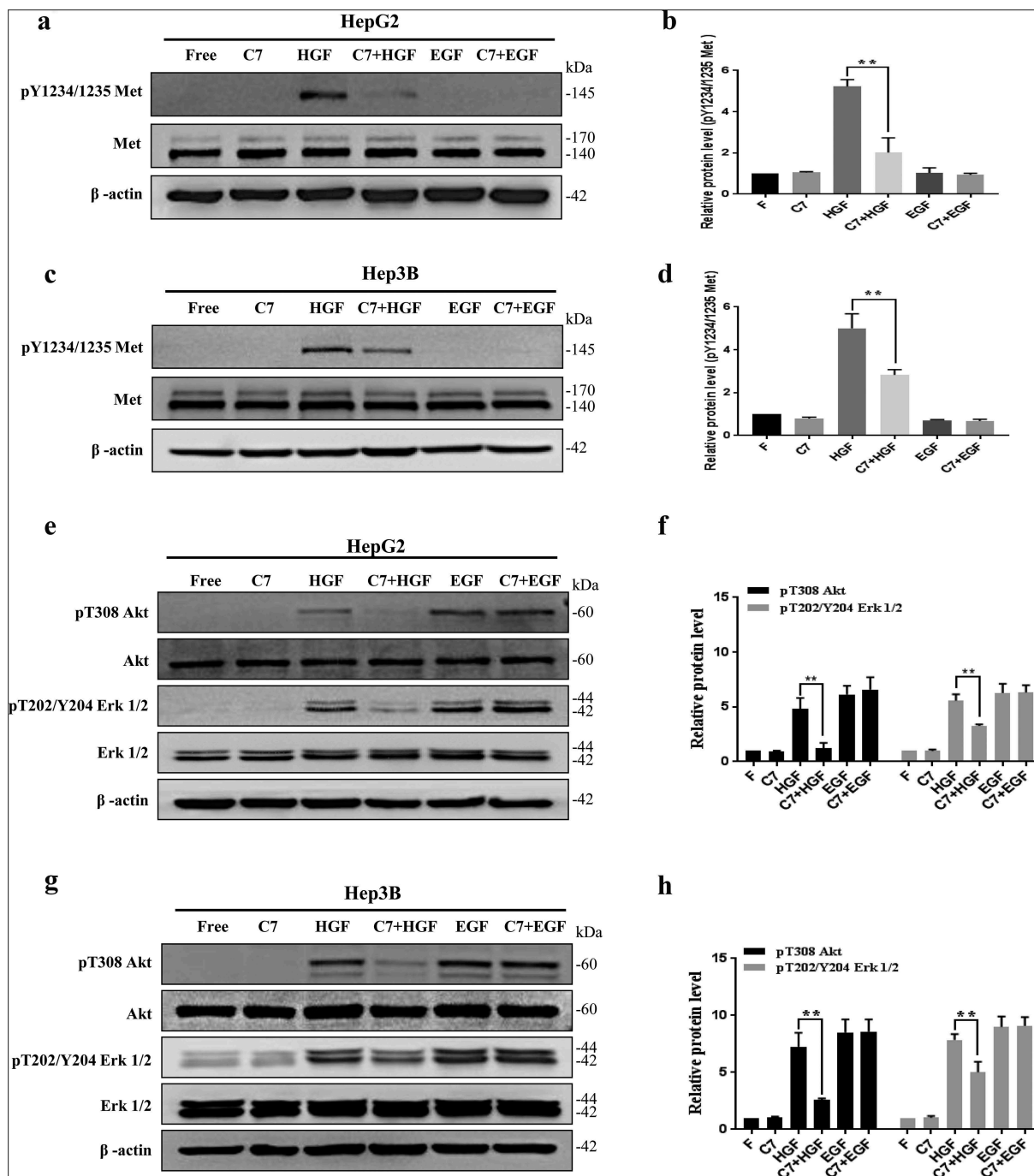


Figure 4. Effect of the C7 peptide on the HGF/c-Met signaling pathway.

(a&c) Western blot analysis of c-Met and phospho-c-Met after 15 min treatment with HGF and EGF in the presence of C7 peptide in HepGH2 and Hep3B cells. (b&d) Statistical analysis result of phospho-Met expression. (e&g) Western blot analysis of Akt, phospho-Akt, Erk1/2 and phospho-Erk1/2. (f&h) Statistical analysis of phospho-Akt and phospho-Erk1/2 expression. F: serum free, C7:100 μ g/ml, HGF: 20 ng/ml, EGF: 10 ng/ml, **P < .01.

water, saline and PBS, which is an advantage that has no toxic effects on cells and mice.

To investigate the inhibition of the C7 peptide in vitro, phosphorylation level of c-Met and its downstream proteins was detected by Western blotting. Phosphorylation of c-Met at Y1234/1235 Y1234, Y1235, Y1349 and Y1356 positively regulate c-Met, which is considered an oncogene involved in cell proliferation, invasion, motility, angiogenesis.³¹ Our results demonstrated that the C7 peptide could inhibit

phosphorylation of c-Met at Y1234/1235. The activation of c-Met can take place by the canonical pathway, which involves HGF binding to c-Met resulting in c-Met homodimerization. In addition to HGF, c-Met can also dimerize with other receptor subunits through noncanonical pathways.³¹ In the canonical pathway, binding of HGF and c-Met causes homodimerization of c-Met and its autophosphorylation at Tyr1234 and Tyr1235, which is the preliminary step in the intracellular signaling pathway.³² Our competitive inhibition

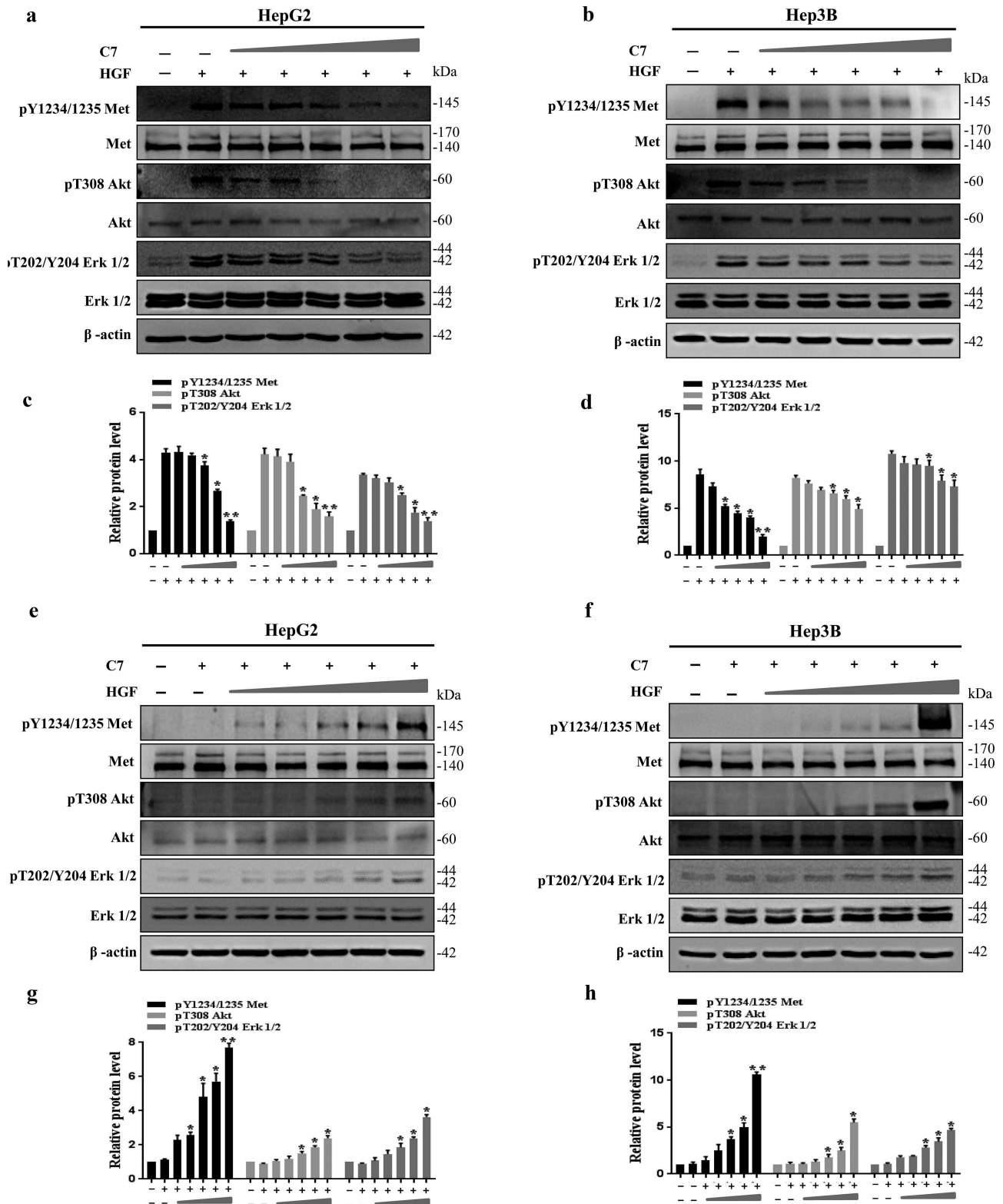


Figure 5. The C7 peptide competitively inhibits the binding of HGF to c-Met.

(a&c) The C7 peptide at different concentrations inhibited the expression of phospho-Met, phospho-Akt and phospho-Erk1/2 induced by HGF. C7 concentration is 0, 0, 20, 50, 100, 150 and 200 μ g/ml, successively. HGF: 20ng/ml. (b&d) Statistical analysis of relative expression of phosphorylated protein, and the second group (HGF group) in each analysis served as a control. (e&g) The C7 peptide inhibited the expression of phospho-Met, phospho-Akt and phospho-Erk1/2 induced by HGF at different concentrations of 0, 0, 5, 10, 20, 40 and 60 ng/ml, successively. C7: 100 μ g/ml. (f&h) Statistical analysis of the relative expression of phosphorylated protein, and the second group (C7 group) in each analysis served as a control. * $P < .05$, ** $P < .01$.

experiments demonstrated that the C7 peptide can block the binding sites of c-Met and HGF, which cannot phosphorylate the c-Met receptor, so that its signal pathway is no longer

transmitted downstream. Although the mechanism by which the C7 peptide blocks the HGF/c-Met signaling pathway has been clearly studied, the docking sites in which C7 interacts

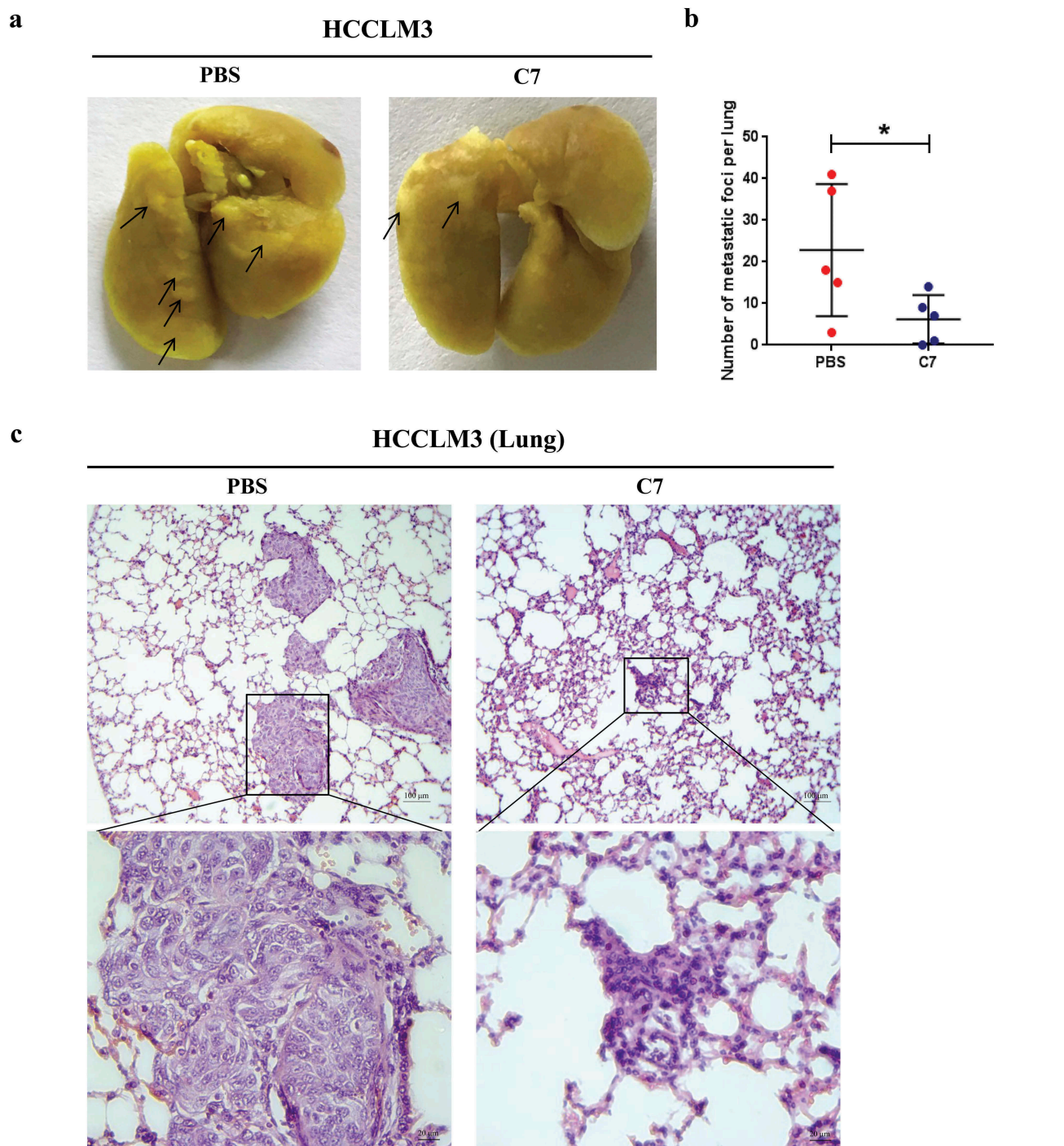


Figure 6. Effect of the C7 peptide on tumor metastasis in the orthotopic xenograft (OX) models.

(a) Photographs of metastatic foci in the lungs of the PBS and C7 groups, C7: 10 mg/kg. (b) The statistical result of the number of metastatic foci in the lungs. (c) Representative photographs of H&E staining in the lungs of nude mice administered PBS or C7.

with the c-Met receptor and the critical amino acid residues that play a key role in the protein binding process remain unknown. If conditions permit, we will explore this further.

Akt and Erk1/2 are significant enzymes in the downstream HGF/c-Met signaling pathway. PI3K/Akt can be activated directly by c-Met and/or indirectly by Ras.³³ In the PI3K/Akt signaling pathway, the binding of growth factors (i.e., HGF and EGF) to their receptors activates PI3K.³⁴ PI3K subsequently produces the formation of phosphatidylinositol-3,4,5-triphosphate, which

activates the serine/threonine kinase Akt to promote tumor cell survival and migration in a multitude of solid tumors.³⁵ In our study, phosphorylation of Akt at Thr308 was inhibited by the C7 peptide to reverse this process. Erk1/2 are ubiquitously expressed hydrophilic nonreceptor proteins that participate in the Ras-Erk cascade.³⁶ Ligand-bound TK receptor such as c-Met would give rise to the activation of Ras-Erk signal transduction cascade and Erk1/2 participated in the regulation of cell motility and invasion.³⁷ Our results showed that the C7 peptide can inhibit

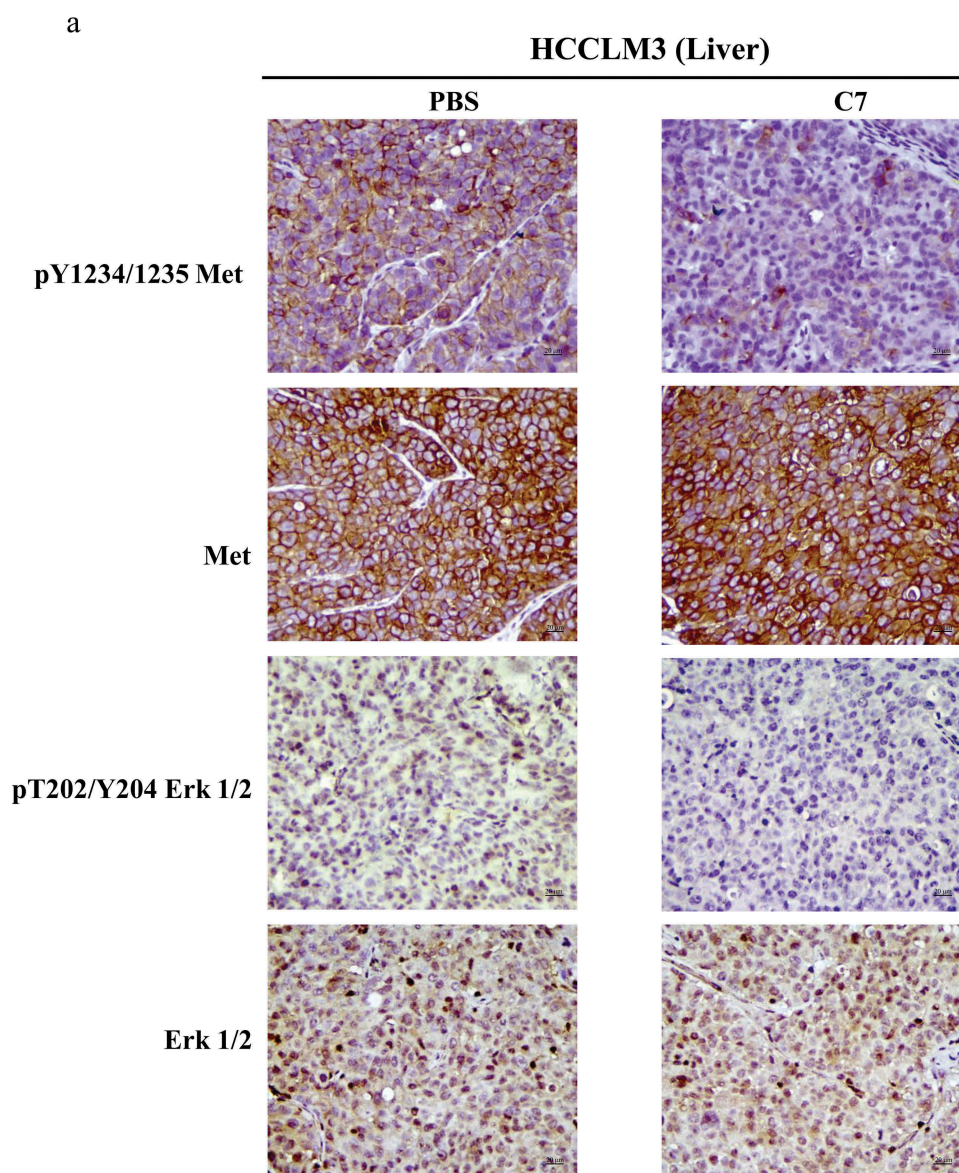


Figure 7. Effect of the C7 peptide on the phosphorylation of both c-Met and Erk1/2 in vivo.

(A) Representative photographs of immunohistological staining using phospho-Met, Met, phospho-Erk1/2 and Erk1/2 antibodies in orthotopic liver tumors of nude mice administered PBS or C7.

the phosphorylation of Erk1/2 deactivating the c-Met receptor. EGF can also activate the Erk1/2 and Akt pathways, which may through EGFR signaling pathway rather than HGF/c-Met signaling pathway. Therefore, C7 peptide did not inhibit EGF-induced activation of the downstream pathway. In this experiment, we concluded that the C7 peptide plays a role in inhibiting cell metastasis by only targeting the HGF/c-Met signaling pathway.

To further confirm whether the C7 peptide actually inhibits the metastasis of hepatocellular carcinoma cells, we designed orthotopic xenograft models. The majority of research papers have used subcutaneous xenograft models to evaluate the effect of drugs,³⁸ but we have used orthotopic xenograft models that are more capable of modeling and can better simulate the tumor metastasis process in vivo.³⁹ HCCLM3 cells first formed a tumor in the liver and then metastasized to the lungs through the blood vessels; subsequently, the C7 peptide attenuated this process. In the later

stages of the animal experiment, one mouse had liquid oozing from the eyes in control group, and we suspected that the mouse occurred brain metastasis. It is reported that brain metastases from HCC are rare, but the incidence is increase in recent years.⁴⁰ In addition, there are no guidelines to treat these patients, but a number of advanced therapeutic techniques have shown an improvement in the median survival time, such as surgical resection and chemotherapeutic agents.⁴¹ This symptom did not occur in the C7 peptide group, so we speculated that the C7 peptide might pass through the blood-brain barrier. This suspicion will further verify in the future. Moreover, two mice were found to have symptoms of ascites in the control group. Clinical data indicated that a large number of patients developing HCC suffer from underlying liver disease, such as ascites, which occurs in up to 56% of patients.⁴² Based on the above information, we considered that the C7 peptide might reduce the incidence of

ascites complications and improved the quality of life of mice. Furthermore, immunohistochemical results showed that the level of phospho-Met and phospho-Erk1/2 in the C7 peptide group was weaker than that of the control group, which was consistent with the results in HepG2 and Hep3B cells. The results in vitro and in vivo further confirmed that the C7 peptide can inhibit tumor metastasis. Certainly, this paper also has some drawbacks. Since there is no mature C7 antibody, the binding of C7 to c-Met cannot be tested by immunofluorescence co-dyeing. The purpose of drug research is ultimately to aid in the clinical use of drugs, so in the next step of this research, we will perform preclinical animal studies to comprehensively evaluate the effect of the C7 peptide.

In summary, we found a c-Met receptor inhibition peptide, named the C7 peptide, that can block the binding sites of HGF and c-Met to inhibit the HGF/c-Met and its downstream signaling pathways, such as the PI3K/Akt and Erk1/2 pathways, to prevent liver cancer metastasis and invasion. Our studies revealed that the C7 peptide represents a promising targeted therapy for treating cancer patients.

Materials and methods

Cells culture

HepG2, Hep3B and HCCLM3 cells were maintained in Dulbecco's Modified Eagle Medium (DMEM, Gibco, California, CA). DMEM was supplemented with 10% fetal bovine serum (FBS Gibco, Australia) and 1% penicillin-treptomycin (SK171206, MRC). All cells were cultured in an incubator (Thermo Fisher Scientific Inc., Massachusetts, USA) at 37°C with 5% CO₂.

Biopanning

Ph.D-C7CTM phage display peptide library kits were purchased from New England Biolabs. The host cells are *E.coli* ER2738. The T7 select Human Liver Tumor cDNA Library was purchased from Novagen Inc. USA. The host cells are BLT5615.

The enzyme-linked plates (Corning, N.Y., USA), coated with the c-Met extracellular domain protein (Sigma, St. Louis, MO) in coating solution (0.1 M NaHCO₃, pH 8.6) at 40 µg/ml, were placed on a refrigerator shaker at 4°C overnight. After the coating solution was removed, the plates were blocked with blocking buffer and incubated at 4°C for at least 1 h. Then, 100 µl phage solution (2×10^{12} /ml) was introduced into each well and incubated for 15–60 min. The plates were washed 6 times with TBS + 0.1% Tween-20 (Sigma) to remove nonspecific phages. The remaining high-affinity phages were eluted with 100 µl of 0.2 mol/L glycine-HCL (pH 2.2), and the eluate was neutralized with 15 µl of 1 mol/ml Tris-HCL (pH 9.1). Four rounds of biopanning were performed, and the eluted high-affinity phages from each round were amplified by incubation with *E.coli* ER2738 host cells. To obtain high-affinity phages, the concentration of the c-Met protein can be appropriately reduced, and the reaction time can be reduced.

Determination of phage titer

A single colony of the *E.coli* ER2738 host cells was inoculated in 5–10 ml Luria-Bertani medium (LB medium) and was grown in a shaker to logarithmic growth phase (OD₆₀₀ ≈ 0.5) at 37°C. The mixture (containing 10 µl of the diluted phage solution, 200 µl of the ER2738 bacterial solution and 3 ml of top agarose) was poured into a prewarmed LB/IPTG/X-gal (TaKaRa, Japan) plate at 37°C and incubated for 8–9 h. The plaque count was determined based on the plate with approximately 100 plaques. The number of plaques multiplied by the dilution is the titer-plaque forming unit (pfu) per 10 µl of phage.

ELISA assay

After the enzyme-linked plate was coated with the c-Met extracellular domain in solution (0.1 M NaHCO₃, pH 8.6), 100 µl gradient-diluted phage (screened monoclonal phage or sequencing-identified negative control phage) was introduced to the plate for 1 h at 37°C. Then, HRP/anti-M13 monoclonal conjugate (Amersham Pharmacia Biotech, Tokyo, Japan), 1:5000 dilution; and TMB (Roche, Mannheim, Germany) were added. The optical density (OD) value at 405 nm was detected by a Varioskan Flash (Thermo Fisher Scientific, Carlsbad, CA).

Peptide preparation

The C7 peptide (Number:04010028654) was synthesized by a twelve-channel and semiautomatic peptide synthesizer (Patent No.: 201020226529.2) by China Peptides Co. Ltd. (Shanghai, China). It was purified (over 99%) and identified by high-performance liquid chromatography (HPLC) and mass spectrometry (MS). After freeze drying, the peptides were dissolved in PBS and preserved at –20°C.

Scatter assay

Cells in the logarithmic growth phase were suspended with 0.25% trypsin following two washes with phosphate buffered saline (PBS). The cells were adjusted to 1×10^4 cells/ml with DMEM containing 10% FBS. 200 µl cell suspension was seeded and cultured in a 96-well plate (Corning) at a density of 2000 cells per well. When cells grew in a clump, HGF (294-HG-005, R&D systems, Minneapolis, MN) and, EGF (AF-100–15, PeproTech, Rocky Hill, CT) supplemented with or without C7 peptide were added to the plate. After 16 h, the medium was removed, and the cells were stained with 0.1% crystal violet. A microscope (Zeiss, Oberkochen, Germany) was used to collect the images.

MTT assay

Cells were seeded into 96-well plates (5000 cells/well) for 24h incubation (37°C) in serum supplemented (10% FBS) media. Thereafter, the cells were treated as indicated in serum-reduced (2% FBS) media including HGF or EGF. Of note, C7 peptide were also added into the media for 24–72 h.

Absorbance at 490 nm was measured by a Varioskan Flash (Thermo Fisher Scientific) after the addition of MTT reagent (keygen bio-tech, Nanjing, China) and DMSO solution (Sigma).

Wound healing assay

A total of 3×10^5 cells were cultured in a six-well plate (Corning). When cells were grown to 80 ~ 90% confluence, a gap was introduced by scraping the cells with a P200 pipette tip, and serum-free medium was added. Cells were treated with HGF and EGF alone or coupled with C7 peptide to stimulate migration across the gap and, photographed using a microscope to evaluate migration inhibition at the time points of 0 and 24 h after wounding.

Migration and invasion assays

With a final concentration between 8×10^4 and 1×10^5 , cells in serum-free medium that were starved for 12 h were plated in upper chambers (invasion assays require Matrigel (BD Biosciences, New York, NY) on the bottom of the upper chamber), which were supplemented with HGF and EGF alone or coupled with C7 peptide. The upper chambers were suspended in 24-well plates containing DMEM with 10% FBS. After 20–24 h, the cells in the upper layer of the membrane were wiped off with wet cotton swabs. The cells in the lower layer of the membrane were washed with PBS twice and then stained with 0.1% crystal violet. After drying, the cells were counted under the microscope.

Protein extraction and western blot

A total of 2.5×10^5 cells were cultured in six-well plates. After reaching 70% confluence, the original medium with 10% FBS was discarded and replaced with serum-free medium and then incubated for 48 h. The C7 peptide was first added to the culture medium for 15 min, before HGF and EGF were added to the culture medium for 15 min. After 15 min, the medium was discarded, and cells were washed with cold PBS twice and lysed with RIPA lysis buffer (P0013C, Beyotime, Shanghai, China) supplemented with complete protease and phosphatase inhibitors (Roche). Subsequently, protein samples were separated by electrophoresis and transferred onto a polyvinylidene difluoride (PVDF) membrane (IPVH00010, Millipore, Billerica, MA). The primary antibodies included β -actin (Abcam, Cambridge, UK), 1:5000 dilution; phospho-Met (Try1234/1235), Met (D1C2), phospho-Akt (Thr308), phospho-p44/42 MAPK (Erk1/2) (Thr202/Tyr204), p44/42 MAPK (Erk1/2) (Cell Signaling Technology, Beverly, MA), 1:1000 dilution; and Akt (Santa Cruz, USA), 1:200 dilution. The secondary antibodies included goat anti-mouse IgG and goat anti-rabbit IgG (Protech, Vancouver, WA), 1:5000 dilution.

Orthotopic xenograft (OX) models

For orthotopic xenograft (OX) models, six to eight-week-old female Balb/c nude mice (Nanjing Model Animal Center, China) were used. LM3 cells were plated in a 100 mm culture

dish and suspended with trypsinized medium when the cells reached 80% fusion. The cell concentration was adjusted to 2×10^6 cells in a 40 μ l serum-free DMEM/Matrigel admixture (1:1 volume). At the same time, a 2 cm incision along each nude mouse left rib margin was made in the abdomen under peritoneal anesthesia. The left lobe of the liver was removed and placed on wet gauze, and was inoculated 40 μ l of cell mixture with a microsyringe, then peritoneum and skin were sutured with a 6–0 line. Two days after transplantation, the C7 peptide was injected intravenously every other day, and PBS was used as a control. All mice were sacrificed six weeks later. Their liver tissues were dissected and fixed with 10% formalin neutral fixative (Yulu, Nanchang, China) for 24–72 h, and the lung tissues were fixed with Bouin's Fluid (Sbjbio Life Sciences, Nanjing, China) for 24 h. The number of nodules per lung was calculated. Liver and lung tissues were analyzed by Immunohistochemistry (IHC) and hematoxylin-eosin (H&E) staining, respectively.

In total, 10 Balb/c female mice were housed in a specific pathogen free (SPF) facility and maintained in a temperature- and light (12 h light/dark cycle) -controlled environment. All protocols for animal care were in concert with regulations for National Institutes of Health Guidelines and the Administration of Affairs Concerning Experimental Animals.

Immunohistochemistry

Dehydration and paraffin embedding were performed on the liver cancer tissue that was fixed in 4% buffered neutral formalin. Consecutive sections 3–4 μ m thick were cut and mounted on microscope slides. After removing paraffin with xylene solution, sections were treated with sodium citrate and 0.1% (v/v) H_2O_2 and then incubated overnight at 4°C with the following antibodies: phospho-Met, 1: 320 dilution; Met, 1: 300; Phospho-Erk, 1:400 dilution; Erk, 1:100 dilution. All antibodies were purchased from Cell Signaling Technology, Inc. The secondary antibody, which was biotinylated goat anti-rabbit IgG (ZSGB-BIO, Beijing, China), was incubated for 30 min at 37°C. These sections were developed using a peroxidase substrate kit (DAB, ZSGB-BIO) for 3 min and counterstained with hematoxylin for 2 min. The sections were sealed with neutral balsam and photographed using a microscope.

H&E staining

The lung tissues were fixed in Bouin's Fluid (Sbjbio, Nanjing, China) for 24 h before photographing and embedded and dehydrated consistent with immunohistochemistry protocols. Five coronal sections were taken from both lungs, and each of the sections was sliced into 8 pieces consecutively. The sections were soaked in hematoxylin stain for 15min and in eosin stain for 10 seconds. The pulmonary metastatic nodules were photographed under the microscope.

Statistical analysis

Measurement data were presented as mean \pm standard deviation. Statistical analysis used SPSS 20.1 (IBM Corp. Armonk, NY, USA). Comparisons between pairwise groups were conducted

using unpaired Student's t-test. Histograms and charts were created with GraphPad Prism 7.0 (GraphPad Software Inc. La Jolla, CA, USA). $P < .05$ was considered statistically significant.

Disclosure of Potential Conflicts of Interest

No potential conflicts of interest were disclosed.

Funding

This work was supported by Chinese National "973" Science Foundation, Grant number: [2002CB513100] and National Natural Sciences Foundation of China, Grant number [81772988].

ORCID

Siying Wang  <http://orcid.org/0000-0003-4793-7389>

References

- Siegel RL, Miller KD, Jemal A. Cancer statistics, 2018. *CA Cancer J Clin.* 2018;68:7–30. doi:10.3322/caac.21442.
- Vauthey JN, Klimstra D, Franceschi D, Tao Y, Fortner J, Blumgart L, Brennan M. Factors affecting long-term outcome after hepatic resection for hepatocellular carcinoma. *Am J Surg.* 1995;169:28–34. discussion –5.
- Bosch FX, Ribes J, Diaz M, Cleries R. Primary liver cancer: worldwide incidence and trends. *Gastroenterology.* 2004;127:S5–s16.
- Ma PC, Tretiakova MS, MacKinnon AC, Ramnath N, Johnson C, Dietrich S, Seiwert T, Christensen JG, Jagadeeswaran R, Krausz T, et al. 2008. Expression and mutational analysis of MET in human solid cancers. *Genes Chromosomes Cancer.* 47:1025–1037. doi:10.1002/gcc.20604.
- Zhang Y, Xia M, Jin K, Wang S, Wei H, Fan C, Wu Y, Li X, Li X, Li G, et al. 2018. Function of the c-Met receptor tyrosine kinase in carcinogenesis and associated therapeutic opportunities. *Mol Cancer.* 17:45. doi:10.1186/s12943-018-0796-y.
- Bottaro DP, Rubin JS, Faletto DL, Chan AM, Kmieciak TE, Vande Woude GF, Aaronson SA. Identification of the hepatocyte growth factor receptor as the c-met proto-oncogene product. *Science.* 1991;251:802–804.
- Nakamura T, Nishizawa T, Hagiya M, Seki T, Shimonishi M, Sugimura A, Tashiro K, Shimizu S. 1989. Molecular cloning and expression of human hepatocyte growth factor. *Nature.* 342:440–443. doi:10.1038/342440a0.
- Scagliotti GV, Novello S, von Pawel J. 2013. The emerging role of MET/HGF inhibitors in oncology. *Cancer Treat Rev.* 39:793–801. doi:10.1016/j.ctrv.2013.02.001.
- Cui JJ. 2014. Targeting receptor tyrosine kinase MET in cancer: small molecule inhibitors and clinical progress. *J Med Chem.* 57:4427–4453. doi:10.1021/jm401427c.
- Jung KH, Park BH, Hong SS. 2012. Progress in cancer therapy targeting c-Met signaling pathway. *Arch Pharm Res.* 35:595–604. doi:10.1007/s12272-012-0402-6.
- Kim KH, Kim H. 2017. Progress of antibody-based inhibitors of the HGF-cMET axis in cancer therapy. *Exp Mol Med.* 49:e307. doi:10.1038/emmm.2017.17.
- Catenacci DVT, Tebbutt NC, Davidenko I, Murad AM, Al-Batran S-E, Ilson DH, Tjulandin S, Gotovkin E, Karaszewska B, Bondarenko I, et al. 2017. Rilotumumab plus epirubicin, cisplatin, and capecitabine as first-line therapy in advanced MET-positive gastric or gastro-oesophageal junction cancer (RILOMET-1): a randomised, double-blind, placebo-controlled, phase 3 trial. *Lancet Oncol.* 18:1467–1482. doi:10.1016/s1470-2045(17)30566-1.
- Abou-Alfa GK, Meyer T, Cheng AL, El-Khoueiry AB, Rimassa L, Ryoo BY, Cicin I, Merle P, Chen Y, Park JW, et al. 2018. Cabozantinib in patients with advanced and progressing hepatocellular carcinoma. *N Engl J Med.* 379:54–63. doi:10.1056/NEJMoa1717002.
- Wang SY, Chen B, Zhan YQ, Xu WX, Li CY, Yang RF, Zheng H, Yue PB, Larsen SH, Sun HB, et al. 2004. SU5416 is a potent inhibitor of hepatocyte growth factor receptor (c-Met) and blocks HGF-induced invasiveness of human HepG2 hepatoma cells. *J Hepatol.* 41:267–273. doi:10.1016/j.jhep.2004.04.013.
- Whittaker S, Marais R, Zhu AX. 2010. The role of signaling pathways in the development and treatment of hepatocellular carcinoma. *Oncogene.* 29:4989–5005. doi:10.1038/onc.2010.236.
- Araste F, Abnous K, Hashemi M, Taghdisi SM, Ramezani M, Alibolandi M. 2018. Peptide-based targeted therapeutics: focus on cancer treatment. *J Control Release.* 292:141–162. doi:10.1016/j.jconrel.2018.11.004.
- Farzaneh Behelgard M, Zahri S, Mashayekhi F, Mansouri K, Asghari SM. 2018. A peptide mimicking the binding sites of VEGF-A and VEGF-B inhibits VEGFR-1/-2 driven angiogenesis, tumor growth and metastasis. *Sci Rep.* 8:17924. doi:10.1038/s41598-018-36394-0.
- Stoker M, Gherardi E, Perryman M, Gray J. 1987. Scatter factor is a fibroblast-derived modulator of epithelial cell mobility. *Nature.* 327:239–242. doi:10.1038/327239a0.
- Giacomin A, Sergio A, Vanin V, Gazzola A, Cazzagon N, Farinati F. 2012. Molecular targeted therapy in hepatocellular carcinoma: present achievements and future challenges. *Dig Dis.* 30:284–288. doi:10.1159/000336993.
- Lee CC, Putnam AJ, Miranti CK, Gustafson M, Wang LM, Vande Woude GF, Gao CF. 2004. Overexpression of sprouty 2 inhibits HGF/SF-mediated cell growth, invasion, migration, and cytokinesis. *Oncogene.* 23:5193–5202. doi:10.1038/sj.onc.1207646.
- Arriola E, Canadas I, Arumi-Uria M, Domine M, Lopez-Vilarino JA, Arpi O, Salido M, Menéndez S, Grande E, Hirsch FR, et al. 2011. MET phosphorylation predicts poor outcome in small cell lung carcinoma and its inhibition blocks HGF-induced effects in MET mutant cell lines. *Br J Cancer.* 105:814–823. doi:10.1038/bjc.2011.298.
- Ogasawara H, Hiramoto J, Takahashi M, Shirahama K, Furusaka A, Hiyane S, Nakada T, Nagayama K, Tanaka T. Hepatocyte growth factor stimulates DNA synthesis in rat pre-neoplastic hepatocytes but not in liver carcinoma cells. *Gastroenterology.* 1998;114:775–781.
- von Schweinitz D, Faundez A, Teichmann B, Birnbaum T, Koch A, Hecker H, Glüer S, Fuchs J, Pietsch T. 2000. Hepatocyte growth-factor-scatter factor can stimulate post-operative tumor-cell proliferation in childhood hepatoblastoma. *Int J Cancer.* 85:151–159. doi:10.1002/(SICI)1097-0215(200011)85:2<151::AID-IJC1>3.0.CO;2-6.
- Maulik G, Shrikhande A, Kijima T, Ma PC, Morrison PT, Sargia R. Role of the hepatocyte growth factor receptor, c-Met, in oncogenesis and potential for therapeutic inhibition. *Cytokine Growth Factor Rev.* 2002;13:41–59.
- Galleo MI, Brier B, Hennighausen L. 2003. Targeted expression of HGF/SF in mouse mammary epithelium leads to metastatic adenocarcinomas through the activation of multiple signal transduction pathways. *Oncogene.* 22:8498–8508. doi:10.1038/sj.onc.1207063.
- Goyal L, Muzumdar MD, Zhu AX. 2013. Targeting the HGF/c-MET pathway in hepatocellular carcinoma. *Clin Cancer Res.* 19:2310–2318. doi:10.1158/1078-0432.CCR-12-2791.
- Boccaccio C, Comoglio PM. 2006. Invasive growth: a MET-driven genetic programme for cancer and stem cells. *Nat Rev Cancer.* 6:637–645. doi:10.1038/nrc1912.
- Knudsen BS, Vande Woude G. 2008. Showering c-MET-dependent cancers with drugs. *Curr Opin Genet Dev.* 18:87–96. doi:10.1016/j.gde.2008.02.001.
- Comoglio PM, Giordano S, Trusolino L. 2008. Drug development of MET inhibitors: targeting oncogene addiction and expedience. *Nat Rev Drug Discov.* 7:504–516. doi:10.1038/nrd2530.
- Chen L, Li C, Zhu Y. 2015. The HGF inhibitory peptide HGP-1 displays promising in vitro and in vivo efficacy for targeted

- cancer therapy. *Oncotarget*. 6:30088–30101. doi:10.18632/oncotarget.3937.
31. Garcia-Vilas JA, Medina MA. 2018. Updates on the hepatocyte growth factor/c-Met axis in hepatocellular carcinoma and its therapeutic implications. *World J Gastroenterol*. 24:3695–3708. doi:10.3748/wjg.v24.i33.3695.
 32. Barbara S, Klaudia S, Marcin M. 2017. Targeting MET receptor in rhabdomyosarcoma: rationale and progress. *Curr Drug Targets*. 18:98–107. doi:10.2174/1389450117666151209124123.
 33. Ponzetto C, Bardelli A, Zhen Z, Maina F, Dalla Zonca P, Giordano S, Graziani A, Panayotou G, Comoglio PM. A multifunctional docking site mediates signaling and transformation by the hepatocyte growth factor/scatter factor receptor family. *Cell*. 1994;77:261–271.
 34. Avila MA, Berasain C, Sangro B, Prieto J. 2006. New therapies for hepatocellular carcinoma. *Oncogene*. 25:3866–3884. doi:10.1038/sj.onc.1209550.
 35. Chen YL, Law PY, Loh HH. Inhibition of PI3K/Akt signaling: an emerging paradigm for targeted cancer therapy. *Curr Med Chem Anti-cancer Agents*. 2005;5:575–589.
 36. Wortzel I, Seger R. 2011. The ERK Cascade: distinct Functions within Various Subcellular Organelles. *Genes Cancer*. 2:195–209. doi:10.1177/1947601911407328.
 37. Sridhar SS, Hedley D, Siu LL. 2005. Raf kinase as a target for anticancer therapeutics. *Mol Cancer Ther*. 4:677–685. doi:10.1158/1535-7163.mct-04-0297.
 38. Tan H, Huang Y, Xu J, Chen B, Zhang P, Ye Z, Liang S, Xiao L, Liu Z. 2017. Spider toxin peptide lycosin-i functionalized gold nanoparticles for in vivo tumor targeting and therapy. *Theranostics*. 7:3168–3178. doi:10.7150/thno.19780.
 39. Du Q, Jiang L, Wang XQ, Pan W, She FF, Chen YL. Establishment of and comparison between orthotopic xenograft and subcutaneous xenograft models of gallbladder carcinoma. *Asian Pac J Cancer Prev*. 2014;15:3747–3752.
 40. Sartori Balbinot R, Facco Muscope AL, Dal Castel M, Sartori Balbinot S, Angelo Balbinot R, Soldera J. 2017. Intraparenchymal hemorrhage due to brain metastasis of hepatocellular carcinoma. *Case Rep Gastroenterol*. 11:516–525. doi:10.1159/000479221.
 41. Rahbari NN, Mehrabi A, Mollberg NM, Muller SA, Koch M, Buchler MW, Weitz J. 2011. Hepatocellular carcinoma: current management and perspectives for the future. *Ann Surg*. 253:453–469. doi:10.1097/SLA.0b013e31820d944f.
 42. Ishizawa T, Hasegawa K, Kokudo N, Sano K, Imamura H, Beck Y, Sugawara Y, Makuuchi M. 2009. Risk factors and management of ascites after liver resection to treat hepatocellular carcinoma. *Arch Surg*. 144:46–51. doi:10.1001/archsurg.2008.511.